Enhanced amorphous stability of carbon-doped $Ge_2Sb_2Te_5$: *Ab Initio* investigation

Eunae Cho, Yong Youn, and Seungwu Han[a)]
Department of Materials Science and Engineering, Seoul National University, Seoul 151-744, Korea

(Received 26 July 2011; accepted 7 October 2011; published online 1 November 2011)

The effects of carbon doping on structural and electronic properties of amorphous $Ge_2Sb_2Te_5$ are studied by using *ab initio* molecular dynamics simulations. In comparison with Si, N, and O dopants, C dopants are found to fundamentally alter the local order of amorphous network by increasing the population of tetrahedral Ge atoms significantly. In addition, the density of ABAB-type squared rings is much smaller than for the undoped case. The present results indicate that carbon dopants are very effective in extending covalent nature in amorphous $Ge_2Sb_2Te_5$ and enhancing amorphous stability. © *2011 American Institute of Physics*. [doi:10.1063/1.3657139]

The phase-change random access memory (PRAM) based on a rapid and reversible crystalline-to-amorphous phase transition of chalcogenide alloys is regarded as a leading contender in the next-generation nonvolatile memory technology.[1,2] Among various chalcogenide alloys, $Ge_2Sb_2Te_5$ (GST) is investigated most intensively as it provides outstanding material properties enabling better stability, speed, and endurance of PRAM. For highly scaled PRAM, however, the material property needs to be tailored further to overcome several technical issues. First, the reset current to amorphize the crystalline phase through melt-quench process should be lowered to reduce power consumption. Second, the thermal interference between neighboring cells requires higher stability of the amorphous phase. Many researchers have been trying to address these issues by incorporating dopants such as N, O, and Si atoms.[3–6] It has been known in optical memories that these dopants stabilize the amorphous phase as signified by increased crystallization temperatures.[7] Recently, we carried out *ab initio* calculations on GST doped with N, O, and Si dopants and investigated the microscopic origin of doping effects.[8] However, the impacts of these dopants on atomic and electronic structures in amorphous GST were found to be modest. This has motivated us to search for a more effective dopant. In this letter, we report that carbon dopants fundamentally affect the amorphous structure in such a way that the stability of the amorphous phase of GST is significantly enhanced.

We use Vienna *ab initio* simulation package (VASP) for molecular dynamics (MD) simulations.[9] The computational parameters are identical to those in Ref. 8. In the crystalline state, we find that the most favorable dopant sites of atomic carbon are interstitial and Te-substitutional sites with insertion energies of 3.59 and 3.62 eV, respectively, when the energy of C atoms is referenced to the carbon graphite. To obtain the carbon-doped amorphous GST (a-CGST), we carry out melt-quench simulations. As an initial configuration, a supercell including 216 atoms of GST and 12 carbon atoms (5.3 at. % doping concentration) is used. The structure is then melted at 2000 K for 12 ps to erase the crystalline bonding network and additionally melted at 1000 K for 30 ps. The liquid structure is subsequently quenched to 300 K with a cooling rate of −15 K/ps. The amorphous structure is obtained by structural relaxation at 0 K including cell shape and volume. For statistical sampling, five amorphous structures are obtained through independent melt-quench simulations. The energy and structural variations among the five a-CGST structures are negligible, and we present results from a specific configuration in the below. For comparison purpose, we also carried out an additional analysis on undoped and N- and O-doped amorphous GST (a-GST, a-NGST and a-OGST, respectively) obtained in Ref. 8.

Figure 1(a) shows the atomic structures of a-CGST. The dopants and surrounding atoms are highlighted with ball-and-stick models. It is found that most carbon dopants are in the sp^3-type tetrahedral geometry with the coordination number of 4. The atom-resolved coordination numbers of C dopants are 1.57, 1.07, and 0.67 on average for Ge, Sb, and Te neighbors, respectively. [For partial pair correlation functions around C atoms, see Fig. S1(a) in supplementary material (Ref. 10).] This bonding preference follows the order of electronegativity difference. In addition, we identify a carbon trimer as marked with a dashed oval in Fig. 1(a). The stable C–C bonds are formed during melt-quench process, and they do not break up during MD simulations even at the melting point of 1000 K. Consistently, the total energy of a-CGST among five configurations tends to be lowered with the increased number of C–C bonds.

In order to understand the structural characteristics of a-CGST, we inspect the local structures around Ge atoms. This is because Ge atoms undergo most dramatic changes upon amorphization or recrystallization.[11] In the crystalline state, Ge atoms are in perfect octahedral configurations (p-bonding), while in the ideal glass which represents the covalent limit of a-GST, they are in tetrahedral geometry (sp^3-bonding).[12] The structure of melt-quenched a-GST lies in between them. The Ge–Te bond lengths in p- and sp^3-bonding geometries are 2.83 and 2.64 Å, respectively, indicating distinct chemical natures.

The partial radial distribution function (PRDF) of Ge–Te bonds is shown in Fig. 1(b). In comparison, PRDFs for a-GST and a-N(O)GST are also displayed. It is found that the Ge–Te bond length read from the peak position is

a)Electronic mail: hansw@snu.ac.kr.

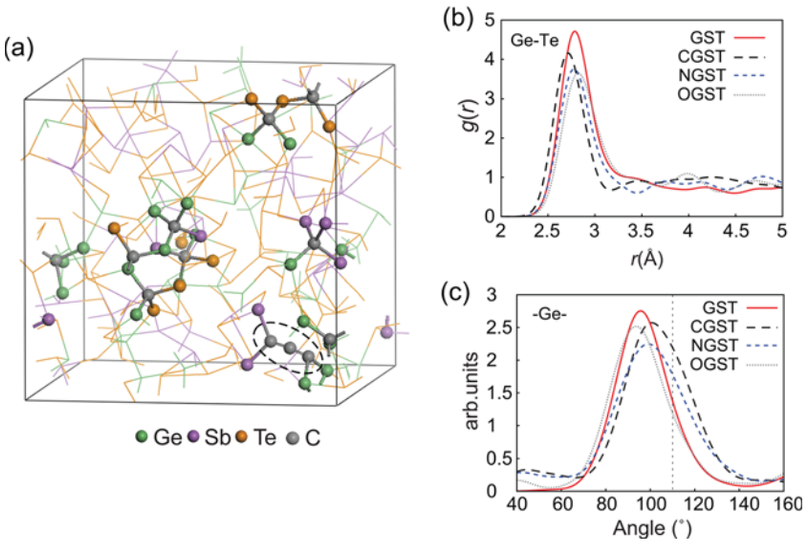

FIG. 1. (Color online) (a) Amorphous structures of CGST. For the visual clarity, only carbon atoms and their neighbors are drawn in ball-and-stick models. (b) The partial radial distribution function [$g(r)$] of Ge-Te. (c) The ADFs around Ge atoms. The vertical dotted line indicates the position of the tetrahedral angle (109.5°).

reduced most significantly for a-CGST, shorter than for a-GST by 0.11 Å. The angle distribution function (ADF) in Fig. 1(c) shows that the peak position shifts to larger angles in a-CGST and a-NGST. However, the spectral weight at the tetrahedral angle (109.5°) in a-CGST is larger than that in a-NGST, meaning that the portion of tetrahedral Ge atoms is the largest in a-CGST. To quantify the concentration of tetrahedral Ge geometrically, we calculate the local order parameter according to Ref. 13 and integrate it between 0.8 and 1.0 to estimate the population of tetrahedral Ge atoms. The percentage of tetrahedral Ge atoms is computed to be 36% in a-GST (among fourfold-coordinated Ge atoms), while the value is increased to 50% in a-CGST.

In Fig. 1(b), it is seen that a new structural feature appears at ~3.5 Å in a-CGST compared to a-GST. This is attributed to the short C–Ge(Te) bonds in Ge-C-Te chains. This is more explicitly shown in the partial radial distribution functions for Ge-Ge and Ge-Sb [see Fig. S1(b) in supplementary material (Ref. 10)], where the peaks around 3.5 Å originate from Ge-C-(Sb,Ge) chains.

The analysis on PRDF and ADF strongly supports that C dopants enhance the covalent nature of GST most significantly among tested dopants. To clarify the origin of pronounced peak shifts in PRDF and ADF of a-CGST, we distinguish two types of Ge atoms; Ge(I) indicates Ge atoms which form bonds with at least one C atom. The other Ge atoms are denoted as Ge(II). The averaged local structures of Ge(I) and Ge(II) are compiled in Table I. For comparison, a similar analysis is also performed for N and O dopants. It is seen that the structural properties for Ge(II) do not vary over dopant types. In contrast, the local order around Ge(I) is sensitive to the dopant type. In particular, the bond length and bond angles of Ge(I) in a-CGST strongly imply that Ge(I) atoms are in a well-defined tetrahedral geometry with the bond length close to that in the ideal glass (2.65 Å).[12] Therefore, C dopants influence neighboring Ge atoms to change chemical order toward sp^3 bonding.

The fast recrystallization of a-GST has been explained by the presence of ABAB-type squared rings (A = Ge or Sb, B = Te) which resemble the structural building block of crystalline GST and, hence, can serve as nucleation sites.[14–16] Therefore, the ABAB squared rings should adversely affect the amorphous stability. In Fig. 2, we examine the distribution of ring structures in amorphous phases. It is noted that even-fold rings are reduced, while odd-fold ones are increased in a-CGST. The inset figure in Fig. 2 shows the number of ABAB squared rings specifically. The suppressed population in a-CGST is most notable. Such a reduction of ABAB rings in the amorphous matrix should slow down nucleation and growth of the crystalline phase, thus significantly enhancing the stability of the amorphous phase. The present results are in line with a recent experiment reporting that carbon doping improved data retention

TABLE I. The coordination numbers, bond lengths, the first peak position of ADF around Ge atoms in amorphous GST structures. Ge(I) atoms are bonded to dopants, while Ge(II) atoms are not.

	Coordination numbers		Bond lengths (Å)		Averaged angle around Ge atoms (°)	
	Ge(I)	Ge(II)	Ge(I)-Te	Ge(II)-Te	-Ge(I)-	-Ge(II)-
a-GST	3.67		2.78		93	
a-CGST	4.00	3.67	2.67	2.74	106	98
a-NGST	4.00	4.00	2.73	2.80	102	95
a-OGST	3.74	3.90	2.84	2.81	98	93

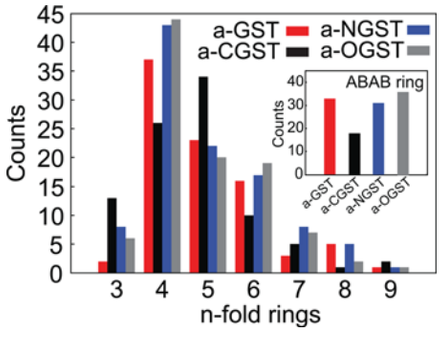

FIG. 2. (Color online) Ring statistics for amorphous GST structures counted per supercell. The inset figure shows the numbers of ABAB-type squared rings.

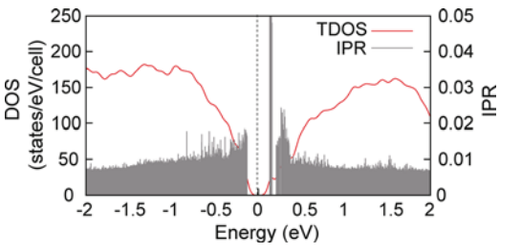

FIG. 3. (Color online) DOS and IPR for a-CGST.

of GeTe phase-changing materials.[17] However, we also note that the insertion energy of C atoms into the crystalline phase is as big as 3.59 eV, which is much larger than 1.91 eV for the amorphous phase. (The insertion energy for the amorphous phase is obtained by averaging five configurations.) This implies that the C atoms might be driven to grain boundaries during recrystallization as has been suggested for N-doped GST.[18,19] This may also contribute to retarding the crystallization speed. Due to the lack of stable Ge-C compound unlike Ge-N phases, the carbon atoms would exist at the grain boundary as cluster forms, rather than compound structures.

In order to understand the reduction of ABAB rings more fundamentally, we calculate the average number of ABAB rings including a specific Ge atom. They are found to be 0.11 and 0.5 for Ge(I) and Ge(II), respectively. In comparison, the corresponding number in a-GST is 0.65. (In the case of Sb atoms, the average number does not depend much on whether C dopants are attached or not.) That is to say, C dopants significantly undermine the formability of four-membered rings of nearby Ge atoms by modifying their chemical nature, which contributes to suppressing ABAB rings in a-CGST.

We calculate the density of states (DOS) and inverse participation ratio (IPR) for a-CGST, as shown in Fig. 3. IPR is determined by the spatial extent over which the wave functions are distributed.[8] For example, IPR is equal to $1/N$ if a specific state is evenly distributed over N atoms. The energy gap of a-CGST read from the band edges in DOS is $\sim$0.3 eV which is similar to that in a-GST. It is noted that IPR increases near valence and conduction band edges in a-CGST, more significantly than a-GST or a-N(O)GST.[8] (From the inspection of spatial distribution of wave functions, it is found that the states at the valence top are mainly lone pairs of Te atoms that are second-nearest neighbors of C dopants.) Therefore, electron localization due to atomic disorder is more severe in a-CGST. This is consistent with the above structural analysis because the covalent nature tends to increase the localization.[12] Lastly, we calculate the optical dielectric constants (ε^{∞}) based on the density-functional perturbation theory. The calculated ε^{∞} of 22 is slightly reduced from 24.5 in a-GST.[8] This is attributed to the increase in covalency of atoms. It is worth noting that the experimental ε^{∞} of a-GST is 16.0,[20] which is much lower than the computed value of 24.5. This would be related to the well-known underestimation of the energy gap by density functional calculations since ε^{∞} for materials with a small band gap is sensitive to the band gap.

This work was supported by the Fundamental R&D Program for Core Technology of Materials and Basic Science Research Program (2010-0011085). Computations were carried out at KISTI (KSC-2010-C2-0011).

[1]A. L. Lacaita and D. J. Wouters, Phys. Status Solidi A **205**, 2281 (2008).
[2]M. H. R. Lankhorst, B. W. Ketelaars, and R. A. M. Wolters, Nat. Mater. **4**, 347 (2005).
[3]B. Liu, Z. Song, T. Zhang, J. Xia, S. Feng, and B. Chen, Thin Solid Films **478**, 49 (2005).
[4]S. Privitera, E. Rimini, and R. Zonca, Appl. Phys. Lett. **85**, 3044 (2004).
[5]B. Qiao, J. Feng, Y. Lai, Y. Ling, Y. Lin, T. Tang, B. Cai, and B. Chen, Appl. Surf. Sci. **252**, 8404 (2006).
[6]J. Feng, Y. Zhang, B. W. Qiao, Y. F. Lai, Y. Y. Lin, B. C. Cai, T. A. Tang, and B. Chen, Appl. Phys. A **87**, 57 (2007).
[7]H. Seo, T.-H. Jeong, J.-W. Park, C. Yeon, S.-J. Kim, and S.-Y. Kim, Jpn. J. Appl. Phys., Part 1 **39**, 745 (2000).
[8]E. Cho, D. Kim, H. Horii, H.-S. Nam, and S. Han, J. Appl. Phys. **109**, 043705 (2011).
[9]G. Kresse and J. Hafner, Phys. Rev. B **47**, 558 (1993).
[10]See supplementary material at http://dx.doi.org/10.1063/1.3657139 for additional figures on the partial radial distribution functions of a-CGST.
[11]A. V. Kolobov, P. Fons, A. I. Frenkel, A. L. Ankudinov, J. Tominaga, and T. Uruga, Nature Mater. **3**, 703 (2004).
[12]E. Cho, J. Im, C. Park, W.-J. Son, D. Kim, H. Horii, J. Ihm, and S. Han, J. Phys.: Condens. Matter **22**, 205504 (2010).
[13]S. Caravati, M. Bernasconi, T. D. Kühne, M. Krack, and M. Parrinello, Appl. Phys. Lett. **91**, 171906 (2007).
[14]J. Hegedus and S. R. Elliott, Nature Mater. **7**, 399 (2008).
[15]J. Im, E. Cho, D. Kim, H. Horii, J. Ihm, and S. Han, Phys. Rev. B **81**, 245211 (2010).
[16]S. Kohara, K. Kato, S. Kimura, H. Tanaka, T. Usuki, K. Suzuya, H. Tanaka, Y. Moritomo, T. Matsunaga, N. Yamada, *et al*., Appl. Phys. Lett. **89**, 201910 (2006).
[17]G. B. Beneventi, E. Gourvest, A. Fantini, L. Perniola, V. Sousa, S. Maitrejean, J. C. Bastien, A. Bastard, A. Fargeix, B. Hyot, *et al*., in *Proceedings of the IEEE International Memory Workshop (IMW)*, Seoul, 2010 (IEEE, N.Y., 2010), p. 21.
[18]R. Kojima, S. Okabayashi, T. Kashihara, K. Horai, T. Matsunaga, E. Ohno, N. Yamada, and T. Ohta, Jpn. J. Appl. Phys. **37**, 2098 (1998).
[19]S. Caravati, D. Colleoni, R. Mazzarello, T. D. Kühne, M. Krack, M. Bernasconi, and M. Parrinello, J. Phys.: Condens. Matter **23**, 265801 (2011).
[20]K. Shportko, S. Kremers, M. Woda, D. Lencer, J. Robertson, and M. Wuttig, Nature Mater. **7**, 653 (2008).